Optics and Lasers in Engineering 71 (2015) 20–32

Contents lists available at ScienceDirect

Optics and Lasers in Engineering

journal homepage: www.elsevier.com/locate/optlaseng

Transport of intensity phase retrieval and computational imaging for partially coherent fields: The phase space perspective

Chao Zuo [a,b,*], Qian Chen [a], Lei Tian [c], Laura Waller [c], Anand Asundi [b]

[a] Jiangsu Key Laboratory of Spectral Imaging & Intelligence Sense, Nanjing University of Science and Technology, Nanjing, Jiangsu Province 210094, China
[b] Centre for Optical and Laser Engineering, School of Mechanical and Aerospace Engineering, Nanyang Technological University, 639798 Singapore
[c] Department of Electrical Engineering and Computer Sciences, University of California, Berkeley, CA 94720, USA

ARTICLE INFO

Article history:
Received 30 September 2014
Received in revised form
6 March 2015
Accepted 6 March 2015
Available online 29 March 2015

Keywords:
Transport of intensity equation
Phase retrieval
Phase space
Partial coherence
Light field imaging

ABSTRACT

The well-known transport of intensity equation (TIE) allows the phase of a coherent field to be retrieved non-interferometrically given positive defined intensity measurements and appropriate boundary conditions. However, in many cases like the optical microscopy, the imaging systems often involve extended and polychromatic sources for which the effect of the partial coherence is not negligible. In this work, we present a phase-space formulation for the TIE for analyzing phase retrieval under partially coherent illumination. The conventional TIE is reformulated in the joint space-spatial frequency domain using Wigner distribution functions. The phase-space formulation clarifies the physical meaning of the phase of partially coherent fields, and enables explicit account of partial coherence effects on phase retrieval. The correspondence between the Wigner distribution function and the light field in geometric optics limit further enables TIE to become a simple yet effective approach to realize high-resolution light field imaging for slowly varying phase specimens, in a purely computational way.

1. Introduction

Phase retrieval is a central problem in many areas of physics and optics because phase carries important information about the object structure and optical properties. For coherent imaging applications, the complete scalar field (amplitude and phase) allows us to achieve beam propagation/manipulation, compute new views at arbitrary perspective, and generate images focused at different depths. However, measuring the phase of an optical field is a challenging issue. Even the fastest detectors available nowadays have integration times that are several orders of magnitude larger than the temporal period of light oscillations. It follows that only the intensity of the field is directly accessible, while any phase information is lost. Although classic interferometric approaches, such as holography and interferometry, allow the phase information to be turned into interference patterns, there also exist non-interferometric phase retrieval techniques that are easier from an implementation point of view. In this paper, we focus on the non-interferometric non-iterative phase retrieval technique based on the transport of intensity equation (TIE) [1]. Without the need of a separate reference beam, the TIE requires only a minimum of two intensity measurements at closely spaced planes for quantitative phase reconstruction. It relaxes the stringent beam-coherence requirements of interferometry and thus extends applications to X-ray diffraction [2], electron-beam microscopy [3], neutron radiography [4], where it is often inevitable or desirable that fields are partially coherent. In addition, in optical phase microscopy, it has been demonstrated that accurate and high-quality quantitative phase imaging can be achieved based on the TIE with partially coherent illuminations, preventing image degradation due to speckle noise [5–10].

The TIE was originally derived by Teague [2] from Helmholtz equation under paraxial approximation. However, Teague's TIE as well as his derivation assumes a monochromatic, coherent beam, which might encounter trouble when dealing with fields exhibiting non-negligible partial coherence. There is no well-defined phase for partially coherent fields, making it necessary to derive more appropriate models of intensity transport for partially coherent, stochastic fields. To this end, some variants of the TIE have been reported to account for the partial coherence explicitly. Streibl [5] extended the Teague's TIE to the general case of partially coherent illumination with the mutual intensity function. He first pointed out the validity of TIE for a spatially partially coherent imaging system, provided that the primary source distribution is symmetric about the optical axis. Paganin and Nugent [11] created a meaningful definition of phase for partially coherent fields using the concept of the time-averaged Poynting vector. Gureyev et al. [12] described an alternative interpretation with the generalized eikonal, based on the spectrum decomposition of a polychromatic

* Corresponding author.
E-mail addresses: surpasszuo@163.com (C. Zuo), chenqian@njust.edu.cn (Q. Chen).

http://dx.doi.org/10.1016/j.optlaseng.2015.03.006
0143-8166/

field. Zysk et al. [13] further explicitly considered the spatially partial coherence with use of coherent mode decomposition, showing that the phase recovered by the TIE is a weighted average of the phases of all modes. Petruccelli et al. [14] developed a partially coherent TIE based on cross-spectral density, allowing removal of coherence-induced phase inaccuracies. In general, these works clarify the meaning of phase and the validity of TIE under partially coherent illuminations from different perspectives. However, most of these treatments presented here employ conventional space–time correlation quantities, like the mutual intensity and the cross-spectral density function, to describe the properties of the partially coherent light. Though these quantities are adequate for the analysis of the propagation and diffraction with light of any state of coherence, their inherent bilinear, stochastic, and wave-optical nature often leads to complicated mathematics and difficulties in comprehension. Notable exception is the Poynting-vector-based interpretation by Paganin and Nugent [11], which establishes the phase of any wave fields (so-called scalar phase), regardless of state of coherence, in terms of the ensemble-averaged probability-current or energy flux density vector. The scalar phase is identical to the conventional phase when the light is coherent, and is still well-defined for partially coherent fields by simply incorporating the ensemble/time average to the Poynting vector. However, the Poynting-vector-based definition is considered more as a conceptual notation rather than a systematic tool for the quantitative analysis of issues (i.e., coherence, aperture effect) related to the TIE phase retrieval.

As an alterative to the space–time correlation functions, a general coherent or partially coherent optical field can be described in terms of light field within geometrical optics [15,16]. The light field has its root in radiometry, representing radiance as a function of position and direction, thereby decomposing optical energy flow along rays. Due to its simplicity and intuitiveness, the ray-based parametrization provides a particularly convenient tool for the design, modelling, and analyzing of optical imaging systems, which is based on purely geometrical rules of ray tracing. In computational photography, recording the light field allows refocusing of the image, or reconstruction of images from different viewing angles after the picture is taken [17]. In the geometrical optics picture, a single ray determines neither a field's amplitude nor phase. The surface of the constant phase is interpreted as wavefronts with geometrical light rays travel normal to them. Their directions coincide with the direction of the ensemble/time-averaged Poynting vector, governed by the eikonal equation within the accuracy of geometrical optics. This is precisely described by the notion of the scalar phase introduced by Paganin and Nugent [11]. However, from a physical point of view, the ray-based light field representation is not a rigorous model and inadequate to describe interference, diffraction, and coherence effects. It is therefore desirable to have a simple mathematical model for the TIE under partially coherent illumination, and providing better understanding of phase retrieval issues by establishing connections between the ray model and more physically correct wave model. Such understanding may lead to further insights to the meaning of the term “phase” of partially coherent fields in such joint context, and facilitate productive exchange of ideas between the fields of TIE phase retrieval and light field imaging.

As an effort to bridge wave optics to rays, phase-space distributions such as the Wigner distribution function (WDF) have been introduced to the study of partially coherent fields [18]. The WDF describes an optical signal in space and spatial frequency (i.e., direction) simultaneously, and can thus be considered a counter-part of the radiance (light field) in wave optics. It represents the field propagation by a simple geometrical relation, i.e., the WDF is constant under propagation along rays. By allowing the possible negativity, the WDF constitutes a rigorous wave-optical foundation for the theory of radiometry [19]. In this work, the TIE phase retrieval is explored systematically under the phase-space framework. We wish to emphasize that the advantages of applying the phase-space representation, i.e., the WDF to reformulate the TIE, are considerable. First, not just limited to coherent optics, the WDF can also serve as a simple, complete, and rigorous description of partially coherent imaging. Such a description will allow us to create a new generalized version of the TIE, yielding an elegant description and intuitive understanding of phase retrieval issues under partially coherent illumination. Second, the phase-space representation enables an explicit and quantitative account of partial coherence and the limited aperture effect from a ‘systems’ view, which clarifies the spatial coherence requirement for the TIE phase retrieval with incoherent source. Thirdly, the natural connection between the WDF and the radiance (light field) not only provides a more physically intuitive picture behind each mathematical formula, but facilitates mutual adaption and extension between the two otherwise unconnected imaging procedures: the TIE and the light field imaging. We emphasize here that we are not the first to apply phase-space quantities to the TIE. A related procedure was previously employed in [20,21] to clarify the uniqueness of the solution, or obtain a simple derivation for the TIE. However, here we first present a systematic phase-space framework of the TIE to clarify its validity in the context of partially coherent imaging, quantify the impacts of the illumination coherence and imaging aperture, and establish its connection with the light field imaging.

The reminder of this paper is outlined as follows. In Section 2, a generalized version of the TIE in phase space is formulated, which explicitly considers the partial coherence state and reduces to Teague's TIE in the limiting case of perfect coherence. In Section 3, we discuss the phase retrieval problem under partially coherent illuminations, and clarify the meaning of phase for a partially coherent field as well as the effect of partial coherence on phase retrieval. In Section 4, the tight connections between the TIE and light field imaging are demonstrated. We show that the phase can be easily recovered from the light field by employing the generalized definition of phase, and conversely, the light field can be retrieved from the TIE for slowly varying objects under certain simplified illuminations. Since no system can achieve perfect imaging in practice, the effect of finite imaging aperture is analyzed and discussed in Section 5. The validating numerical simulations and experiments are presented in Sections 6 and 7, respectively. Finally, this paper is concluded in Section 8.

2. Generalized transport of intensity in phase space for partially coherent fields

The description of partially coherent light by means of space–time correlation functions forms the basis for the definition of the WDF. Let $U(\mathbf{x})$ be a paraxial, temporally stationary, and ergodic scalar field with arbitrary spatial and temporal coherence, where $\mathbf{x}$ is the two-dimensional (2D) spatial vector. The second-order coherence properties of the field may be expressed in terms of the mutual coherence function:

$$\tilde{\Gamma}(\mathbf{x}_1,\mathbf{x}_2,\tau)=\langle U(\mathbf{x}_1,t)U^*(\mathbf{x}_2,t+\tau)\rangle, \tag{1}$$

where the sharp bracket denotes the ensemble average, which is equivalent to a time-average, taken over the interval of a single realization of the field. The temporal power spectrum of the mutual coherence function

$$\Gamma(\mathbf{x}_1,\mathbf{x}_2,\omega)=\int \tilde{\Gamma}(\mathbf{x}_1,\mathbf{x}_2,\tau)\exp(i2\pi\omega\tau)\,d\tau, \tag{2}$$

called cross-spectral density (CSD), plays a central role in the classic coherence theory since it describes the ensemble-averaged

correlations of a given monochromatic component (characterized by the optical frequency $\omega = c/\lambda$, where c is the speed of light and λ is the wavelength) of the whole field. Note that all integrals in this paper are performed over the entire range of the integration variable. Next, we prefer to convert the CSD to the WDF in 4D phase space $(\mathbf{x}, \mathbf{u})$, through a Fourier transform in the differential space variable $\mathbf{x}'$:

$$W_\omega(\mathbf{x}, \mathbf{u}) = \int \Gamma\left(\mathbf{x}+\frac{\mathbf{x}'}{2}, \mathbf{x}-\frac{\mathbf{x}'}{2}, \omega\right) \exp(-i2\pi \mathbf{u}\mathbf{x}')\, d\mathbf{x}', \tag{3}$$

where $\mathbf{u}$ is the spatial frequency vector corresponding to $\mathbf{x}$. The advantages of the phase-space formulation in terms of the WDF are three-fold. First, due to the statistical nature of the WDF, we can incorporate the partial coherence of the field in more compact formula. Second, mathematically the WDF is much easier to handle than the CSD due to its affine canonical covariance in phase space. Finally, the WDF closely resembles the ray concept in geometric optics, providing an intuitive and insightful interpretation of the physical picture behind each result. The power spectral density of the wave field is given by the space marginal of the WDF:

$$S(\mathbf{x}, \omega) = \Gamma(\mathbf{x}, \mathbf{x}, \omega) = \int W_\omega(\mathbf{x}, \mathbf{u})\, d\mathbf{u}. \tag{4}$$

The paraxial propagation of the WDF obeys the Liouville transport equation [18] in phase space:

$$\frac{\partial W_\omega(\mathbf{x}, \mathbf{u})}{\partial z} + \lambda \mathbf{u} \cdot \nabla_{\mathbf{x}} W_\omega(\mathbf{x}, \mathbf{u}) = 0, \tag{5}$$

whose solution takes the form

$$W_\omega(\mathbf{x}, \mathbf{u}, z) = W_\omega(\mathbf{x} - \lambda z \mathbf{u}, \mathbf{u}, 0), \tag{6}$$

where z is the propagation distance. Integrating Eq. (5) over all spatial frequencies and combining the definition of the power spectral density given by Eq. (4), we can find that

$$\frac{\partial S(\mathbf{x}, \omega)}{\partial z} = -\nabla_{\mathbf{x}} \cdot \int \lambda \mathbf{u} W_\omega(\mathbf{x}, \mathbf{u})\, d\mathbf{u}, \tag{7}$$

where $\nabla_{\mathbf{x}}$ is the 2D gradient operator over $\mathbf{x}$. Eq. (7) can be regarded as the transport of spectrum equation for polychromatic fields. It relates the longitudinal evolution rate of the optical power spectral density to the transverse divergence of the first frequency moment of the WDF. The time-averaged intensity of a partially coherent beam coincides with the integral of the power spectral density over all optical frequencies [12,13]. Hence, we integrate Eq. (7) over ω to obtain a new version of the TIE:

$$\frac{\partial I(\mathbf{x})}{\partial z} = -\nabla_{\mathbf{x}} \cdot \iint \lambda \mathbf{u} W_\omega(\mathbf{x}, \mathbf{u})\, d\mathbf{u}\, d\omega. \tag{8}$$

Note that the only assumption employed in deriving Eq. (8) is the paraxial field to be temporal stationary and ergodic; thus, it is general enough to cover various optical fields with arbitrary spatial and temporal coherence. We will call Eq. (8) the generalized transport of intensity equation (GTIE) to differentiate it from the conventional TIE derived by Teague. Now let us consider a few important special cases of the GTIE: first, when the field is quasi-monochromatic, i.e., the field consists of almost a single optical frequency, the spectral density $S(\mathbf{x}, \omega)$ is simply the intensity. In this case, the field can be regarded as almost completely temporally coherent. Thus, the transport of spectrum equation reduces to the GTIE for spatially partially coherent fields:

$$\frac{\partial I(\mathbf{x})}{\partial z} = -\lambda \nabla_{\mathbf{x}} \cdot \int \mathbf{u} W(\mathbf{x}, \mathbf{u})\, d\mathbf{u}. \tag{9}$$

Note that although the temporal coherence of the illumination can be simply incorporated by the integral over all optical frequencies as in Eq. (8), it should be stressed that for dispersive samples, the inherent wavelength-dependent refractive index often complicates the accurate phase determination. For the remainder of this paper, we will drop the spectral dependence ω (assuming quasi-monochromaticity) for simplicity, but it should be noted that for polychromatic fields, the WDF characterizes only a single spectral component of the whole field. However, quasi-monochromatic fields still are not necessarily deterministic due to the statistical fluctuations over the spatial dimension. This randomness can be removed by further limiting the field to be completely spatially coherent as well. Then the field becomes deterministic and can be fully described by the 2D complex amplitude $U(\mathbf{x}) = \sqrt{I(\mathbf{x})} \exp[i\phi(\mathbf{x})]$, where $\phi(\mathbf{x})$ is the phase of the completely (both temporally and spatially) coherent field. From the time(space)–frequency analysis perspective, the completely coherent field can be regarded as a mono-component signal, and the first conditional frequency moment of the WDF (instantaneous frequency) is related to the transverse phase gradient of the complex field [22,23]:

$$\frac{\int \mathbf{u} W(\mathbf{x}, \mathbf{u})\, d\mathbf{u}}{\int W(\mathbf{x}, \mathbf{u})\, d\mathbf{u}} = \frac{1}{2\pi} \nabla_{\mathbf{x}} \phi(\mathbf{x}). \tag{10}$$

Substituting Eq. (10) into Eq. (9) leads to Teague's TIE:

$$\frac{\partial I(\mathbf{x})}{\partial z} = -\frac{1}{k} \nabla_{\mathbf{x}} \cdot \left[I(\mathbf{x}) \nabla_{\mathbf{x}} \phi(\mathbf{x}) \right]. \tag{11}$$

This equation is a second-order elliptic partial differential equation, which provides a simple and deterministic method for phase retrieval from intensity measurements. Provided the intensity distribution is strictly positive, the phase can be uniquely determined (up to an arbitrary additive constant) by solving the equation with appropriate boundary conditions [20,24]. As is shown, the validity of Teague's TIE is restricted to fully coherent fields, while the GTIE, which is a generalized version of the TIE in phase space, explicitly considers the coherence states so that it can be applied to a much wider range of optical- and electron-beams. Note that a similar version of Eq. (9) was originally introduced by Gureyev et al. [20] based on Walther's generalized radiance function (see Eq. (7) of Ref. [20]), which turned out to be mathematically equivalent to the WDF. And later Semichaevsky and Testorf [21] extended it to coherent phase retrieval in terms of the ambiguity function. While the phase-space quantities were employed in these previous work, here we first present a systematic phase-space framework of the TIE to clarify its validity in the context of partially coherent imaging, quantify the impacts of the illumination coherence and imaging aperture, and establish its connection with the light field imaging, as will be detailed below.

3. Phase retrieval under partially coherent illumination

One difficulty in extending the GTIE to phase retrieval arises from the fact that the partially coherent field does not have a well-defined phase since the field experiences statistical fluctuations over time. However, the phase-space representation on the LHS of Eq. (10) is still valid, leading to a new meaningful and more general definition of "phase". Here we refer the new "phase" $\tilde{\phi}(\mathbf{x})$ defined by Eq. (10) as the generalized phase of partially coherent fields to distinguish it from its coherent counterpart. It can be seen from Eq. (10) that the generalized phase is a scalar potential whose gradient yields the conditional frequency moment of the WDF. It is clear from a distribution point of view that the quantity is the average spatial frequency at a particular location. In the optical context, the simultaneous space–frequency description of the WDF is analogous to what is known as the radiance, which describes the amount of energy each ray carries [19]. Thus, $W(\mathbf{x}, \mathbf{u})$ can be intuitively interpreted as the energy density of the ray travelling through the point $\mathbf{x}$ and having a frequency (direction) $\mathbf{u}$. Eq. (6) exactly represents the geometric-optical behavior of a ray travelling through free space [25], and Eq. (4) implies that the intensity at a point is simply the sum of the energy spreading over all possible directions. More importantly, the frequency moment of the WDF, $\int \mathbf{u} W(\mathbf{x}, \mathbf{u})\, d\mathbf{u}$,

represents the transversal ensemble/time-averaged flux vector (transversal time-averaged Poynting vector) [23,26]. The ratio of the time-averaged flux vector to the intensity (so-called normalized average flux/Poynting vector) gives the time-averaged directions of the energy flow. Thus Eq. (10) suggests that the time-averaged flux lines are defined as the orthogonal trajectories to the generalized phase (or wavefront), they coincide with the direction of the average Poynting vector. This is in precise accordance with the notion of the scalar phase introduced by Paganin and Nugent [11]. However, it should be noted that the WDF is not a rigorous energy density function (radiance function) due to its possibility for negativeness. The negative values of the WDF originate from the phase space interference [27], and can trace back to the uncertainty principle in optics [28], allowing the description of coherent effects, such as interference and diffraction. However, no problems are encountered when the WDF is used to represent other quantities that can be measured. For example, the WDF marginal projections used in Eq. (10), which give measurable quantities (intensity, time-averaged Poynting vector), are always non-negative. Furthermore, in the case of low spatial coherence where coherent interference effects statistically wash out, or a coherent field with a slowly varying wavefront (which will be discussed in Section 4), one can safely interpret the WDF as an energy density without worrying about the negativity.

We are now ready to explore the possible application of the generalized TIE for phase retrieval for partially coherent fields. It should be emphasized that the major concern in such scenario is the well-defined phase shift introduced by the specimen, rather than the generalized phase of the partially coherent field itself. This leads to the natural choice of treating the contributions of the incident illumination and specimen separately by considering the transmitted field as a product of the illumination function $U_{in}(\mathbf{x})$ and the sample transmission function $T(\mathbf{x})=\tau(\mathbf{x})\exp[i\phi(\mathbf{x})]$, where $\tau(\mathbf{x})$ and $\phi(\mathbf{x})$ are the amplitude and the phase of the specimen, respectively. The CSD of the resultant field just leaving the object can be written as $\Gamma_{out}(\mathbf{x}_1,\mathbf{x}_2)=T(\mathbf{x}_1)T^*(\mathbf{x}_2)\Gamma_{\text{in}}(\mathbf{x}_1,\mathbf{x}_2)$. Substituting it into the definition of the WDF [Eq. (3)] and using the convolution theorem of the Fourier transform, we can represent the overall WDF as a convolution of the object transmittance WDF, $W_T(\mathbf{x},\mathbf{u})$, and the illumination WDF, $W_{in}(\mathbf{x},\mathbf{u})$, over the spatial frequency variable:

$$W_{out}(\mathbf{x},\mathbf{u})=W_T(\mathbf{x},\mathbf{u})\underset{\mathbf{u}}{\otimes}W_{in}(\mathbf{x},\mathbf{u})=\int W_T(\mathbf{x},\mathbf{u}')W_{in}(\mathbf{x},\mathbf{u}-\mathbf{u}')\,d\mathbf{u}'. \tag{12}$$

Substituting Eq. (12) into the LHS of Eq. (10) and interchanging the order of integral, it can then be derived that the generalized phase of the transmitted field, $\tilde{\phi}_{out}(\mathbf{x})$, should satisfy the following expression (the proof is given in Appendix A):

$$\frac{\int \mathbf{u}W_{out}(\mathbf{x},\mathbf{u})\,d\mathbf{u}}{\int W_{out}(\mathbf{x},\mathbf{u})\,d\mathbf{u}}=\frac{\int \mathbf{u}W_T(\mathbf{x},\mathbf{u})\,d\mathbf{u}}{\int W_T(\mathbf{x},\mathbf{u})\,d\mathbf{u}}+\frac{\int \mathbf{u}W_{in}(\mathbf{x},\mathbf{u})\,d\mathbf{u}}{\int W_{in}(\mathbf{x},\mathbf{u})\,d\mathbf{u}}, \tag{13}$$

or equivalently,

$$\nabla_{\mathbf{x}}\tilde{\phi}_{out}(\mathbf{x})=\nabla_{\mathbf{x}}\left[\tilde{\phi}_{in}(\mathbf{x})+\phi(\mathbf{x})\right]. \tag{14}$$

This representation shows the generalized phase accrues upon propagation through the object, behaving precisely as a conventionally defined phase. The total generalized phase is the sum of the phase of the object and the generalized phase of the incident illumination. In general, the determination of the object phase requires two independent measurements, performed with and without the presence of the specimen. The sample-free measurement is used to characterize $\tilde{\phi}_{in}(\mathbf{x})$ of the incident beam and is subsequently subtracted from the total generalized phase $\tilde{\phi}_{out}(\mathbf{x})$ to get the net phase introduced by the object only. This is similar to the schemes suggested by Gureyev et al. [29] and Petruccelli et al. [14], which employ additional experiment to remove the influence of the non-flat "phase" of the incident illumination. However, if the illumination is chosen judiciously to directly nullify $\tilde{\phi}_{in}(\mathbf{x})$,

$$\int \mathbf{u}W_{in}(\mathbf{x},\mathbf{u})\,d\mathbf{u}=0. \tag{15}$$

The total generalized phase $\tilde{\phi}_{out}(\mathbf{x})$ directly gives $\phi(\mathbf{x})$ and one single measurement is sufficient to recover the object phase even though the illumination is not fully coherent. The null frequency moment condition given in Eq. (15) suggests that the time-averaged flux lines of the illumination should be all parallel to the optical axis (no transversal flux, or the transversal flux vectors cancel out in the ensemble average). For purely coherent illuminations, Eq. (15) simply means the local wavefront is flat, which includes the case of on-axis plane wave, and the waist of a Gaussian beam. For partially coherent spatially stationary illuminations [18], which will be generally true for the experimental arrangements in optical microscopy since they typically use Köhler illumination geometry, the spatially incoherent primary source (usually in the condenser aperture plane for an optical microscope) featured by the intensity distribution $|P_c(x)|^2$ and the positional CSD $\Gamma(\mathbf{x}+\mathbf{x}'/2,\mathbf{x}-\mathbf{x}'/\mathbf{x}'2)=|P_c(x)|^2\delta(\mathbf{x}')$ is collimated by the condenser (or simply propagated to the far field), producing the illumination WDF $W_{in}(\mathbf{x},\mathbf{u})$ just before the object plane:

$$W_{in}(\mathbf{x},\mathbf{u})=|P_c(\mathbf{u})|^2. \tag{16}$$

Eq. (16) is in fact an expression of the Van Cittert–Zernike theorem. Note that the above expression ignores the constant coordinate scaling factor associated with the Fourier transform pair, which is trivial when all computations are carried out in normalized units. Substituting Eq. (16) into Eq. (15) reveals that the primary source distribution must be symmetric about the optical axis, which corresponds to the case discussed by Streibl [5] and Petruccelli et al. [14].

Before proceeding further, we must emphasize that though the GTIE is derived in the joint space-spatial frequency domain using WDF, here we do not intend directly to apply the GTIE [Eqs. (8)–(10)] for phase retrieval because the WDF is difficult to measure directly (though it can be approximately measured by using a microlens array [30] or indirectly measured through the phase-space tomography [31,32], for phase retrieval these methods are not recommended due to the low spatial resolution and experimental complexity). The main point to be conveyed here is that phase retrieval can be realized by directly applying the original Teague's TIE [1,24] for partially coherent fields, by adopting the new generalized TIE and the generalized definition of "phase" that is valid for partially coherent fields. In other words, for completely coherent fields, if we take the axial intensity derivative and then solve Teague's TIE, we obtain the phase of the field; for partially coherent fields, by following the same procedure, we obtain the generalized phase of the partially coherent field instead. Since the conditional frequency moments of the WDF are additive [Eq. (13)], the gradient of the generalized phase also is additive [Eq. (14)]. Hence, the generalized phase of the transmitted field can be decomposed into the generalized phase of the incident illumination plus the phase shift introduced by the specimen. This decomposition is unique up to an unimportant constant that may float between the two components. The GTIE itself knows nothing about the object phase and the generalized phase of the illumination, it only recovers the generalized phase of the total beam after passing through the object. However, our objective is to determine the well-defined phase shift introduced by the specimen rather than the "phase" of the illumination or the total transmitted partially coherent field. To resolve this problem, one needs to either separate the two terms with two independent measurements explicitly, or directly nullify the "phase" of the illumination. As discussed above, for the coherent imaging, an

illumination with flat wavefront is required; and for spatial stationary illuminations, the primary source distribution must be symmetric about the optical axis. In fact, for the completely coherent case, such kind of treatment has been habitually adopted in TIE literature. For spatial stationary illuminations, it is also quite easy to realize in practice, e.g. the built-in Köhler illumination in a normal bright-field microscope (of course, the condenser aperture must be properly centered on the optical axis, which is usually clearly explained in the microscope operating manual).

Actually, such treatment is conceptually somewhat similar with the two beam interferometry, where the phase measured is the phase difference between the object beam and the reference beam. Without any pre-knowledge about the reference beam and the object illumination, one can never get the phase of the object itself with only single measurement. Therefore, normally the illumination and the reference beam of an interferometer are designed to generate perfect plane wave (or spherical wave for measuring spherical wavefront) so that the phase of the object can be obtained through a single measurement. Alternatively, if the system is not perfectly designed or aligned, one can use the famous double exposure scheme (with sample-free images) [33] to remove all the aberrations in the imaging system and extract the phase of the object only. These methods and concepts are quite similar to the GTIE measurement.

4. Computational light field imaging for slowly varying phase specimens

In this section, we will establish connections between the TIE phase retrieval and light field imaging. Essentially, the two imaging procedures look for complete descriptions of the properties of a field, but from different perspectives. Light field (radiance) represents all possible light rays in the field as a 4D function of position and direction, while for coherent imaging applications, the 2D complex field encodes the position and direction information in its amplitude and phase. The 2D intensity and phase give total knowledge about the complex field so that the behavior of the field can be perfectly predicted. Such complete knowledge permits various forms of coherent optical imaging systems, such as the Zernike phase contrast and differential interference contrast imaging to be computationally emulated without resorting to actual optical hardware [34,35]. Obviously, the 4D phase-space representation of a coherent field is highly redundant because the complex field is defined only over the 2D plane. This phase-space redundancy leads to a highly localized WDF, but usually accompanied with oscillations (include negative values) due to the phase-space interference contributions. As we discussed in Section 3, this interference effect can be accounted by giving up the requirement that the radiance to be positive for all rays, which makes little physical sense but converts rays to be a useful tool for modelling wave effect [19,36,37]. Alternatively, to keep its physical meaning of radiance (the amount of light carried by each ray), one must allow the existence of the "usual rays", whose trajectories deviate from straight lines near regions with significant interference effect (e.g. focal regions) [38]. To avoid such complexities, in the following we assumes the object is slowly varying with $\mathbf{x}$ that terms of ≥ 3 order in the Taylor expansion can be ignored (which is also one validity condition the TIE generally required). In this case, the phase-space oscillations disappear (the diffraction effect can be neglected) and the WDF occupies only a single slice in phase space (the proof is given in Appendix B):

$$W(\mathbf{x},\mathbf{u}) = I(\mathbf{x})\delta\left[\mathbf{u} - \frac{1}{2\pi}\nabla\phi(\mathbf{x})\right]. \tag{17}$$

The WDF given above now is non-negative and perfectly localized in phase space, taking on all the properties of radiance. It clearly describes that the geometrical light ray at single position travels only along single direction described by the phase normal (coincides with the direction of the Poynting vector). It also tells us that the total amount of light carried by each ray is described by the intensity of the field. This is an advantageous feature to allow phase measurement simply by measuring the directions of rays, e.g. the Shack–Hartmann sensor [39]. Fig. 1 visualizes a smooth coherent wavefront and its corresponding WDF and light field representation, with the simple relation $\theta = \lambda\mathbf{u}$ connecting the spatial frequency and the ray angle.

The situation becomes more complex when the field is not strictly coherent. Generally, the phase-space WDF constitutes a rigorous and non-redundant description for partially coherent fields. The knowledge of amplitude and (generalized) phase are not sufficient to determine the full field unambiguously [20,40]. Yet another approach, known as phase-space tomography, can recover the full 4D WDF based on extensive intensity measurements at a range of propagation distances (with symmetry-breaking elements inserted in the beam path) [31,32]. The negativity and oscillations problem can be significantly reduced or even disappears if the field exhibits significant spatial incoherence (as shown in Section 3, the spatial coherence tends to smooth the coherent WDF along the frequency dimension), and then the WDF again approaches to the radiance or the light field. From the geometric optics perspective, for each point on the beam there exist many geometric rays with different directions; they fan out to make a 2D distribution, which accounts for the higher dimensionality of the partially coherent field. The light field camera, as a counterpart of the Shack–Hartmann sensor in the computer graphics community, allows joint measurement of the spatial and directional distribution of light [17]. Light field imaging enables us to apply ray-tracing techniques to compute synthetic photographs, depth estimation, flexibly change the focus and perspective view. However, it requires elaborate optical setups

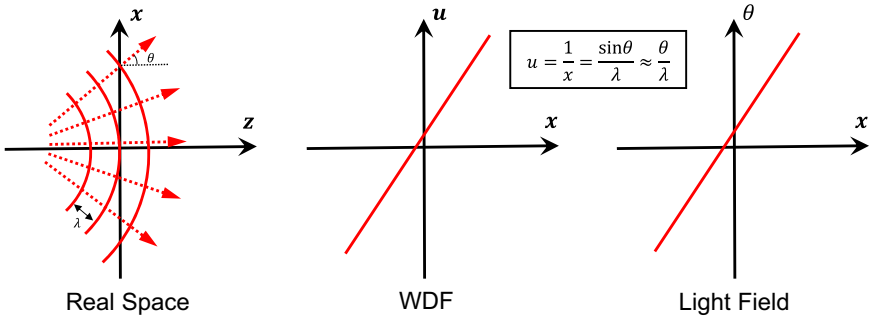

Fig. 1. Visualization of a smooth coherent wavefront and its corresponding WDF and light field. The phase is represented as the localized spatial frequency (instantaneous frequency) in the WDF representation. Rays travel perpendicular to the wavefront (phase gradient).

and significantly sacrifices spatial resolution (traded for angular resolution) as compared to conventional imaging technique.

We now consider the potential connections between the TIE phase retrievaland light field imaging. As is shown by Eq. (10), the phase of the field (regardless of its state of coherence), which is a scalar potential whose gradient yields the conditional frequency moment of the WDF, can be retrieved from the TIE with a minimum of two closely spaced intensity measurements. Applying the approximation $L(\mathbf{x},\theta)\approx W(\mathbf{x},\lambda\mathbf{u})$ to Eq. (10), we can describe the phase in terms of the light field:

$$\frac{\int \theta L(\mathbf{x},\theta)\,d\theta}{\int L(\mathbf{x},\theta)\,d\theta}=k^{-1}\nabla\phi(\mathbf{x}). \tag{18}$$

This equation shows that the phase gradient is related to the normalized transverse average energy flux vector. The well-defined energy flux density vectors are weighted and averaged at a single location to form a unique and also well-defined average flux vector. Put simply, the quantity on the LHS is just the centroid of the light field – the average direction of light at one given position. Eq. (18) clearly reveals that a standard TIE measurement can provide important (though not complete) information of the light field, at least its angular marginal and first angular moment. Conversely, it also tells us that the phase gradient can be easily recovered from the 4D light field by a simple centroid detection scheme. This is similar with the standard procedure in the Shack–Hartmann method. The only possible difference is that for coherent wavefronts, geometrical light ray at single position travels only along single direction, so the Shack–Hartmann sensor forms a focus spot array sensor signal. While for partially coherent fields, geometric rays at a single position travel in various directions, forming a 2D sub-aperture image array instead.

It would be interesting to consider the question we left at the end of [41]. Though generally the TIE measurement is inadequate to fully characterize the partially coherent field (or the light field), in certain situations (besides the completely coherent case), we can indeed fully characterize the optical field without the need of measuring the whole phase-space distribution. A simple yet practical case has already been presented in an earlier section of this paper: a slowly varying specimen under spatially stationary illumination. Substituting Eqs. (16) and (17) [for $W_T(\mathbf{x},\mathbf{u})$] into Eq. (12) and applying the approximation $L(\mathbf{x},\theta)\approx W(\mathbf{x},\lambda\mathbf{u})$, we obtain

$$L(\mathbf{x},\theta)=cI(\mathbf{x})\left|P_c\left[\theta-k^{-1}\nabla_{\mathbf{x}}\phi(\mathbf{x})\right]\right|^2, \tag{19}$$

where c is a constant ensuring $I(\mathbf{x})=\int L(\mathbf{x},\theta)\,d\theta$. As shown in Fig. 2, Eq. (19) represents exactly the geometric optical behavior of the specimen: for each incident ray, it leaves the specimen from the same location, but its direction is shifted as a function of the phase gradient of the object. The specimen can be regarded as a spreadless or angle-shift invariant system: it does not change the angular spread of the incident rays, which is fully determined by the source intensity distribution. To retrieve the light field, one has to know the radiances and directions of rays fanning from each object point. From Eq. (19), we know that with the knowledge of the source intensity distribution, the object intensity (directly measurable) and phase (can be retrieved using the TIE with a minimum of two intensity measurements), the 4D light field can be fully characterized, with no other effort to look for other projections of the 4D WDF. Interestingly, Eq. (19) also provides a meaningful interpretation of the empirical Gaussian angular distribution assumption made by the recently reported light field moment imaging technique [42] – it represents the special case that the primary source distribution of the spatially stationary illumination is Gaussian.

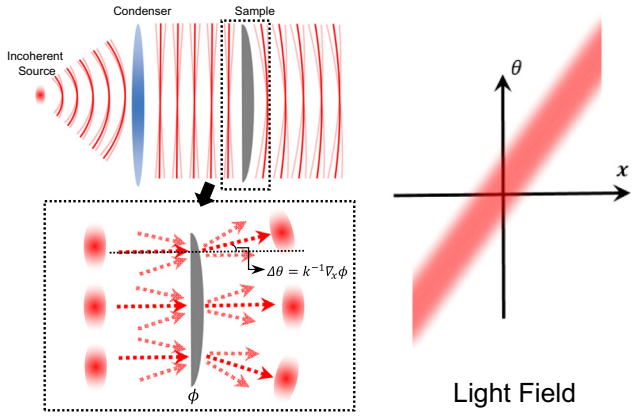

Fig. 2. Light field representation of a slowly varying object under spatially stationary illumination. The sample exhibits angle-shift invariance: at each location, the direction of each incident ray shifts by the amount of object phase gradient.

5. Finite aperture effect of imaging systems

Another important assumption made in TIE is perfect imaging which is not fulfilled in a practical imaging system, such as a microscope. In fact, what we measure is the phase of the field in the image plane, which is not exactly the phase of the object itself, especially when the pupil of the imaging system is insufficient to transmit all spatial frequencies of interest in the object. In this case, understanding and quantifying the effect of the imaging system appears particularly important. Consider a practical imaging system with a finite aperture, the CSD in the image plane can be written as

$$\Gamma_{image}(\mathbf{x}_1,\mathbf{x}_2)=\Gamma_{out}(\mathbf{x}_1,\mathbf{x}_2)\underset{\mathbf{x}_1,\mathbf{x}_2}{\otimes}h(\mathbf{x}_1,\mathbf{x}_2), \tag{20}$$

with the mutual point spread function (PSF) $h(\mathbf{x}_1,\mathbf{x}_2)$ defined as

$$h(\mathbf{x}_1,\mathbf{x}_2)=h(\mathbf{x}_1)h^*(\mathbf{x}_2), \tag{21}$$

where $h(\mathbf{x})$ is the coherent PSF of the imaging system. With the convolution theorem, the corresponding WDF of the wave field in the image plane can be written as

$$\begin{aligned}W_{image}(\mathbf{x},\mathbf{u})&=\int\Gamma_{image}\left(\mathbf{x}+\frac{\mathbf{x}'}{2},\mathbf{x}-\frac{\mathbf{x}'}{2}\right)\exp(-i2\pi\mathbf{u}\mathbf{x}')\,d\mathbf{x}'\\&=W_{out}(\mathbf{x},\mathbf{u})\underset{\mathbf{x}}{\otimes}W_{psf}(\mathbf{x},\mathbf{u})\\&=W_T(\mathbf{x},\mathbf{u})\underset{\mathbf{u}}{\otimes}W_{in}(\mathbf{x},\mathbf{u})\underset{\mathbf{x}}{\otimes}W_{psf}(\mathbf{x},\mathbf{u}).\end{aligned} \tag{22}$$

It is seen that the effect of the imaging system is equivalent to convolving the WDF of imaging PSF over the spatial variable $\mathbf{x}$. More importantly, $W_{psf}(\mathbf{x},\mathbf{u})$ is zero when $\mathbf{u}$ falls outside of the pupil (in most cases the pupil function is equal to a circ-function, i.e., $P(\mathbf{u})=1$, $|\mathbf{u}|\le u_{NA}$ and $P(\mathbf{u})=0$, $|\mathbf{u}|>u_{NA}$), which means all WDF components outside the pupil will be dumped by the imaging system. Since the TIE retrieves the conditional frequency moment of the WDF as the phase gradient

$$\frac{1}{2\pi}\nabla_{\mathbf{x}}\phi_{image}(\mathbf{x})=\frac{\int\mathbf{u}W_{image}(\mathbf{x},\mathbf{u})\,d\mathbf{u}}{\int W_{image}(\mathbf{x},\mathbf{u})\,d\mathbf{u}}, \tag{23}$$

the reconstructed phase in the image plane does not coincident with the true phase of the object in general (expect for the case of perfect imaging, i.e., $P(\mathbf{u})=1$, and the $W_{psf}(\mathbf{x},\mathbf{u})$ reduces to $\delta(\mathbf{x})$). Due to the bilinear nature of image formation in partially coherent imaging systems, such kind of phase discrepancy is difficult to analyze or compensated directly. However, once again if we consider a slowly varying specimen under spatially stationary

illumination, Eq. (22) can be further simplified as

$$W_{image}(\mathbf{x},\mathbf{u}) \approx cI(\mathbf{x})\left|P_c\left[\mathbf{u}-\frac{1}{2\pi}\nabla_{\mathbf{x}}\phi(\mathbf{x})\right]\right|^2 |P(\mathbf{u})|^2. \quad (24)$$

Thus, the reconstructed gradient of the generalized phase in the image plane is the frequency centroid of the overlapping area of the shifted primary source and the pupil function. Without considering the effect of the imaging system, the phase gradient is just the centroid of the shifted primary source. As long as the source distribution is symmetric with respect to the optical axis, the phase can be accurately retrieved, regardless of the source size (spatial coherence of the illumination). However, in a practical imaging system, it is necessary to give a higher importance to the illumination coherence, because the size of the light source has a significant influence on the imaging. Though decreasing the source size does helps improve the phase retrieval accuracy (better linear transfer for lower phase gradient), it will compromise the resolution limit. Furthermore, a certain degree of illumination coherence is necessary. For incoherent imaging (the source size is larger than the pupil) the real frequency centroid corresponding to the object phase gradient can never be correctly identified by the TIE due to the apodization effects of the pupil function. For partially coherent imaging (the source size smaller than the pupil), the imaging system induced phase distortion still exists, but can be further compensated. However, this point is beyond the scope of our current work and subject to further exploration.

Applying the ray approximation $L(\mathbf{x},\theta) \approx W(\mathbf{x},\lambda\mathbf{u})$, the physical picture behind Eq. (24) becomes quite clear. The angular distribution of the light field just leaving the object is determined by the source intensity distribution shifted by the amount of the phase gradient of the object. The imaging system only allows rays with the angles within the pupil ($|\theta| \le \lambda u_{NA}$) to pass and blocks the rest with larger angles. The intensity finally captured in the image plane is the sum of all rays passing through the imaging system, determined by the overlapping area of the shifted primary source and the pupil function:

$$I_{image}(\mathbf{x}) = cI(\mathbf{x}) \int \left|P_c\left[\mathbf{u}-\frac{1}{2\pi}\nabla_{\mathbf{x}}\phi(\mathbf{x})\right]\right|^2 |P(\mathbf{u})|^2 \, d\mathbf{u}. \quad (25)$$

This equation is quite useful to recreate 2D images of the object from arbitrary perspectives: with the retrieved phase gradient $\nabla_{\mathbf{x}}\phi(\mathbf{x})$, one can simply synthesize different views through Eq. (25) by shifting the position of the primary source P_c artificially. Compared with the method presented in [42] (so-called pinhole renderings as in traditional light field imaging), which constructs the 4D light field first and then extracts its 2D slices as perspective-shifted 2D images, Eq. (25) employs no empirical assumptions and gives a more physically meaningful way for high-resolution view synthesis with the effect of the imaging system taken into account.

6. Numerical simulations

To illustrate the proposed theory, we have performed a series of numerical simulations. As shown in Fig. 3(a), the simulated object is a pure phase sinusoidal grating with three different periods, 3 μm, 1.5 μm, and 0.75 μm. To visualize the phase-space quantities more conveniently, the sinusoidal grating is represented by a 1D signal, as shown in Fig. 3(b). The object is illuminated by Köhler illumination with a disk-shaped condenser aperture ($NA_{cond} = 0.3$), and the illumination intensity uniformly distributed over the aperture plane. The wavelength of the quasi-monochromatic illumination is $\lambda = 550$ nm. The object is then imaged with an objective with $NA_{obj} = 0.7$, thus the coherent diffraction limit of the system is 0.7863 μm and 1.27 μm^{-1}. All computations are performed in normalized units of λ/NA_{obj} for the space coordinate and NA_{obj}/λ for the spatial frequency coordinate. As shown in Fig. 3(c) and (d), in normalized coordinates, the radii of the P_c and P are S and 1, respectively, where S is the so-called the coherence parameter, which is the ratio of condenser to objective numerical apertures (S=0.42857). The inverse Fourier transform of the objective pupil gives the coherent PSF of the imaging system, which is shown in Fig. 3(e).

Fig. 4(a) shows the WDF of the specimen $W_T(\mathbf{x},\mathbf{u})$ computed from the object transmittance. According to Eq. (10), the phase derivative obtained through the TIE is equal to the first conditional frequency moment of the WDF. To verify the accuracy of phase retrieved by TIE, we compared its derivative with the ideal phase derivative calculated from the original phase function, shown in the normalized range from $[-1, 1]$ [Fig. 4(b)]. The perfect match between the two curves indicates that the phase can reliably be recovered by the TIE for the completely coherent case. We next examine the case when the specimen is illuminated by the partially coherent Köhler illumination, but assuming perfect imaging conditions. According to Eq. (12), the WDF at the object plane $W_{out}(\mathbf{x},\mathbf{u})$ can be calculated by convoluting the WDF of the object transmittance $W_T(\mathbf{x},\mathbf{u})$ with the illumination WDF $|P_c(\mathbf{u})|^2$, as illustrated in Fig. 4(c). Compared with Fig. 4(a), the blurring of WDF along the frequency dimension is clearly seen in Fig. 4(d). However, due to the symmetry of the condenser aperture $|P_c(\mathbf{u})|^2$, this blurring does not change the frequency centroid of the object WDF, thus the phase derivative can still be accurately retrieved, as verified by Fig. 4(e).

We next examine the case when the illustration is asymmetric about the optical axis [Eq. (15) is thus not satisfied]. As shown in Media 1, we intentionally shift the condenser aperture along coordinate to induce the asymmetry of the light source (off-axis illumination). The retrieved phase derivative deviates from the ideal value by a constant as expected. In this case, the frequency centroid of incident illumination WDF $|P_c(\mathbf{u})|^2$ [the second term on the RHS of Eq. (13)] needs to be characterized in the absence of the specimen. It can then be subtracted to remove the influence of illumination and recover the phase derivative induced by the specimen only.

Finally, the effect of the imaging system is considered. The WDF of the imaging PSF, $W_{psf}(\mathbf{x},\mathbf{u})$, is shown in Fig. 4(f), and according to Eq. (22) the image plane WDF $W_{image}(\mathbf{x},\mathbf{u})$ can be calculated by convoluting $W_{out}(\mathbf{x},\mathbf{u})$ with $W_{psf}(\mathbf{x},\mathbf{u})$ along the $\mathbf{x}$-direction, as shown in Fig. 4(g). The imaging system removes all the WDF component falling outside of the pupil ($|\mathbf{u}| \le 1$), which in turn causes blurring in the retrieved phase derivative, as shown in Fig. 4(h). The imaging PSF greatly reduces the phase contrast of the 0.75 μm grating, but the phase structure for lower spatial frequencies is less affected. It is instructive to further examine the effect of the illumination coherence (i.e., the effect of gradually changing the condenser aperture) when the imaging PSF is considered. The associated Media 2 shows above quantities calculated at $S = 0.01$–2. These coherence parameters range from almost completely coherent to incoherent illumination and demonstrate remarkably the effect of the coherence on the resolution of the reconstructed phase gradient. When the illumination is almost coherent $S < 0.1$, the 0.75 μm grating is smoothed out since it is beyond the coherent diffraction limit. As the coherence parameter increases, the 0.75 μm grating can be slightly resolved due to the increase in the diffraction limit, while the accuracy of the 1.5 μm grating is compromised. With the further increase in S, the strength of all the gratings, including the 3 μm, one begin to reduce. In particular, the resolvability of all gratings is greatly attenuated when the value of S reaches 0.8, and finally smoothes out as S approaches 1. These results confirm that though the TIE itself does not impose any requirement on the illumination coherence, for a practical imaging system, a certain level of spatial

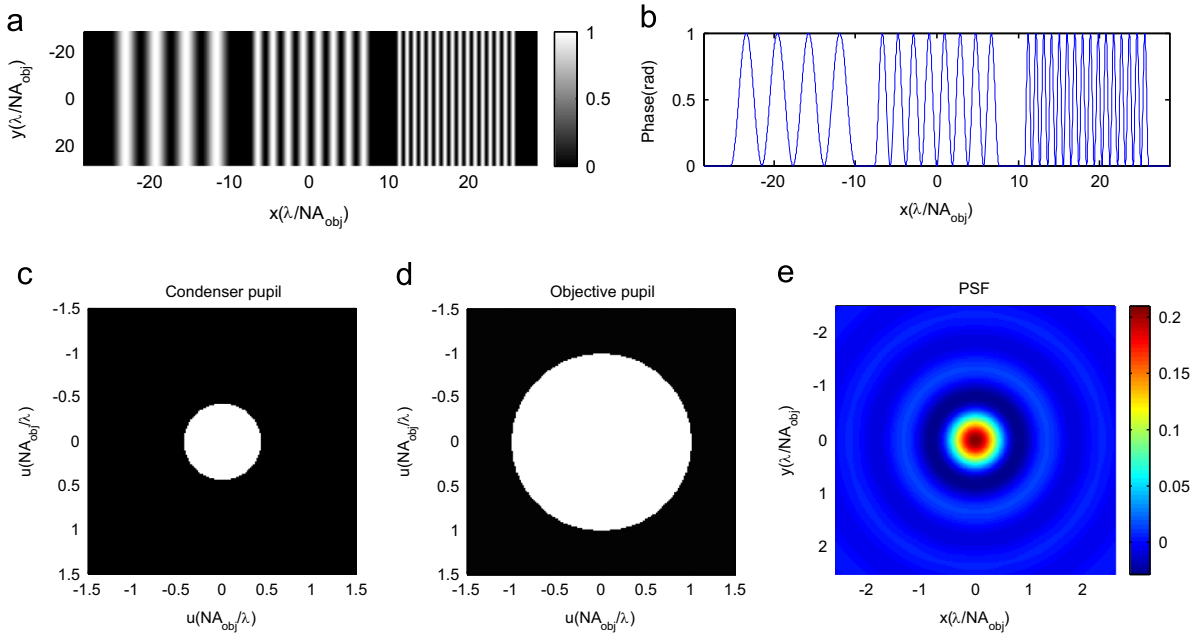

Fig. 3. Numerical simulation on a pure phase sinusoidal grating. (a) Phase distribution of the simulated object. (b) 1-D profile of the phase function. (c) Condenser pupil function. (d) Objective pupil function. (e) The coherent PSF of the imaging system. All axes are expressed in the normalized units.

coherence of the illumination is indispensable, and narrowing down the condenser aperture a bit ($S = 0.3$–0.4) does help us to improve the phase retrieval performance.

7. Experimental results

7.1. Phase retrieval under partially coherent illumination

The correctness and validity of the proposed theory has been verified through a series of experiments. Recent applications of the TIE under partially coherent illuminations have already confirmed that the quantitative phase can be accurately retrieved without stringent beam-coherence requirements [6,11,10,35]. Thus, we only show one special phase retrieval experiment to demonstrate the importance of the null frequency moment condition given by Eq. (15). The experimental configuration used for the present study is based on (but not limited to) a tunable lens based TIE (TL-TIE) system, described in detail in [35]. The sample measured is a plano-convex quartz microlens array with 250 μm pitch, imaged via a 10 × objective with 0.25 NA. A rectangular aperture is introduced in the intermediate image plane of the microscope to generate the required boundary conditions for solving the TIE with the fast discrete cosine transform (DCT) solver [24,43]. The illumination from the built-in halogen lamp is filtered by an interference filter with a central wavelength of 550 nm and a bandwidth of 45 nm. We fabricate one disk-shaped aperture ($NA_{cond} = 0.1$) and put it into the condenser turret. The transverse position of the aperture can be easily changed and we centered it with respect to the optical axis at first to make sure that Eq. (15) is established. In this case, the phase of the microlens is nicely reconstructed, as shown in Fig. 5(a). The result is validated by benchmarking against the white-light scanning confocal microscopy (Sensofar PLμ, 50 × $NA_{obj} = 0.8$). The relative difference between the two methods is less than 1%, which suggests that it is clearly possible to perform a high-precision TIE phase measurement even though the illumination is partially coherent and the conventional idea of the phase is broken down. However, if we shift the condenser aperture horizontally so that the center of the aperture does not coincide with the optical axis, an off-axis tilt phase aberration is superimposed on the original phase, as shown in Fig. 5(b). The result is in accordance with our simulation result. As suggested in Section 3, such tilt aberration can be numerically compensated with double exposure scheme (with sample-absent image) or the digital phase mask as widely used in digital holographic microscopy [33,44,45].

7.2. From light field to phase

The above experiment demonstrated that phase information can be quantitatively retrieved from a set of defocused images through solving the TIE. However, acquiring the through-focus image stack is usually time-consuming, as the sample stage or camera has to be moved between image captures. Though several configurations have been developed to eliminate the mechanical motion [7,35,10], the light field imaging enables a totally new way to collect the entire image stack in single capture, as the intensity images at an arbitrary focal plane can be computationally reconstructed from the raw light field image [17]. This undoubtedly suggests one viable way to convert the light field to the phase.

An alternative way to reconstruct the phase from the light field, as we discussed in Section 4, is to apply the definition of the generalized phase [Eq. (18)] directly. The generalized phase at the geometric optics limit can be regarded as the centroid of the light field – the average direction of light at one given position, suggesting that the phase gradient can be easily recovered by a simple centroid detection scheme applied to the raw light field image. Compared to the first method, which first reconstructs the through-focus stack, then solves the TIE explicitly; the second method, which employs the definition of the generalized phase here, is inherently much easier and straightforward.

A typical example to verify to correctness of Eq. (18) is shown. The experiment is based on a light field microscope [built upon a conventional microscope (Olympus BX41) with a microlens array (pitch 150 μm, ROC 10.518 mm) inserted in the intermediate image plane just before the camera sensor]. The sample is a plano-convex microlens array (pitch 100 μm), which is imaged with a 20 × objective with $NA_{obj} = 0.4$. Four light field images with the condenser NA from 0.05 to 0.25 are recorded, as shown in Fig. 6. From the enlarged images, we can clearly see the intensity

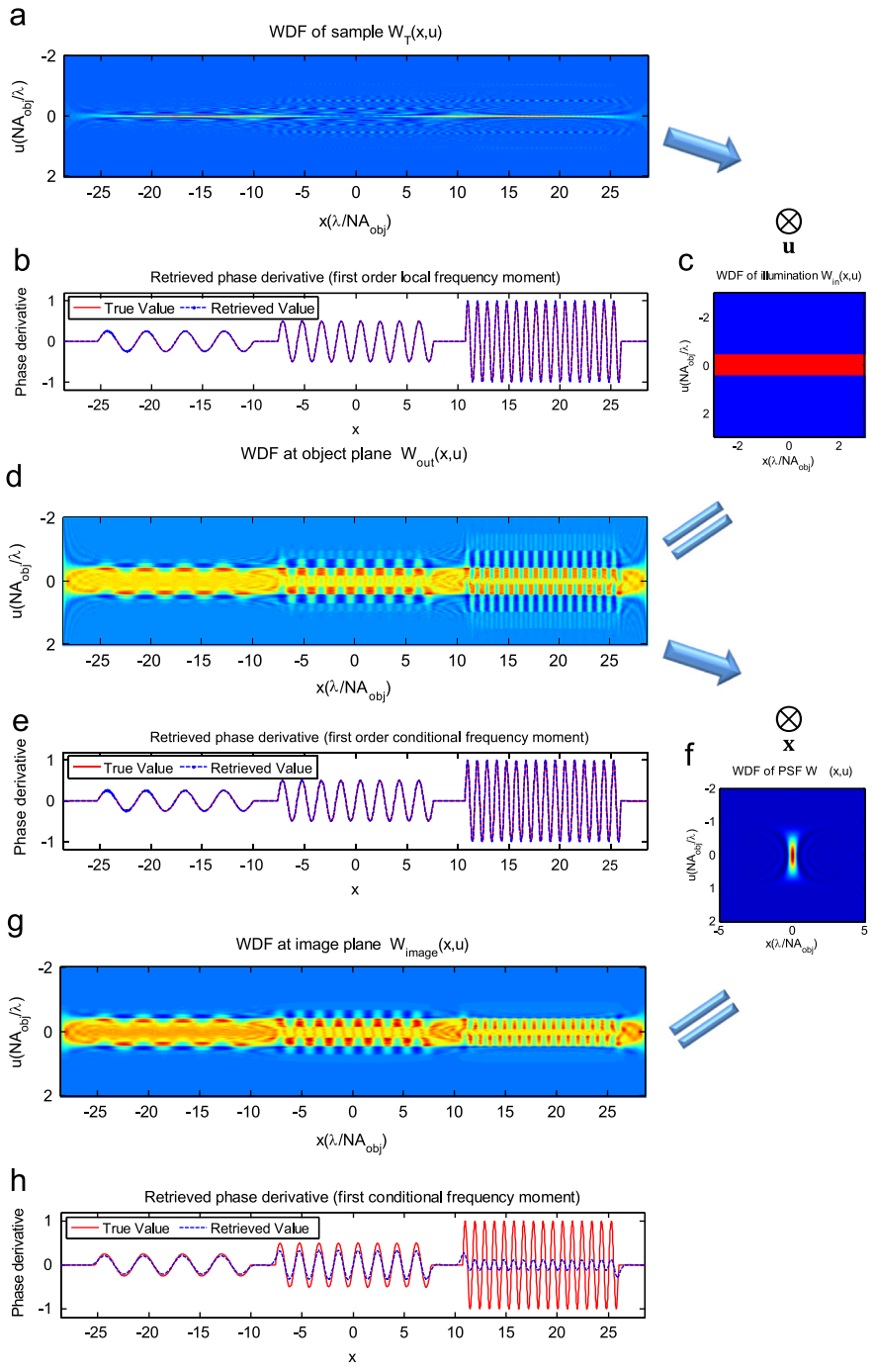

Fig. 4. (Media 1, Media 2) Phase-space description of the effects of illumination and imaging system on the TIE phase retrieval. See the text for details. (a) WDF of the specimen; (b) retrieved phase derivative from (a); (c) WDF of the illumination; (d) WDF of the field in object plane; (e) retrieved phase derivative from (d); (f) WDF of the PSF of the imaging system; (g) WDF of the field in image plane; (e) retrieved phase derivative from (g).

changing corresponding to each lenslet, from a focus spot array to a 2D sub-aperture image array. The centroid for each sub-image is calculated, followed by an integration to reconstruct the phase, as shown in Fig. 7. The results confirm that the phase can be extracted from the light field; even though the beam is not completely coherent. Note that when the condenser aperture is open up to $NA_{cond} = 0.25$, the sub-aperture images are too large causing them to overlap, which causes problems for the centroid locating, resulting in artifacts in the final reconstructed phase image. In Fig. 8, we show another example to examine the validity of Eq. (18) for a more complex sample (stem cells). The phase is recovered but at lower spatial resolution inherent in light field camera imaging. Fig. 8(c) shows the phase after cubic interpolation with less mosaic effect. These results prove the correctness of Eq. (18), showing that the quantitative phase information can be directly extracted from the WDF (light field). However, this method for phase retrieval is not recommended due to the lower spatial resolution and the experimental complexity as compared to the full-resolution TIE technique.

7.3. From phase to light field

In last subsection, it was shown that phase can be recovered from light field images since the 4D light field has a higher

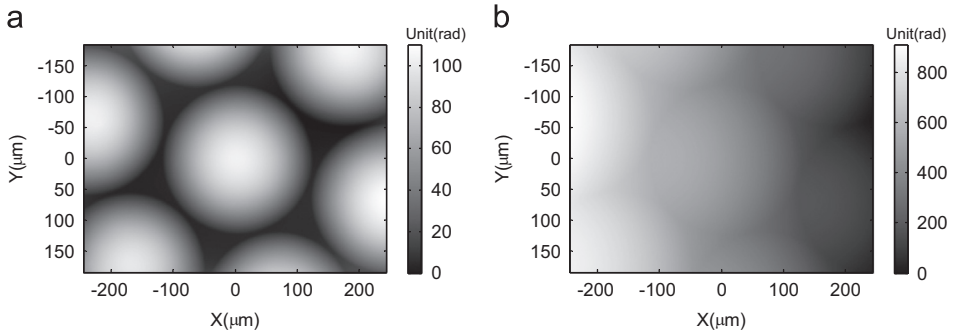

Fig. 5. Characterization of a plano-convex quartz microlens array. (a) Retrieved phase when the aperture is centered on the optical axis; (b) retrieved phase when the condenser aperture is off-axis.

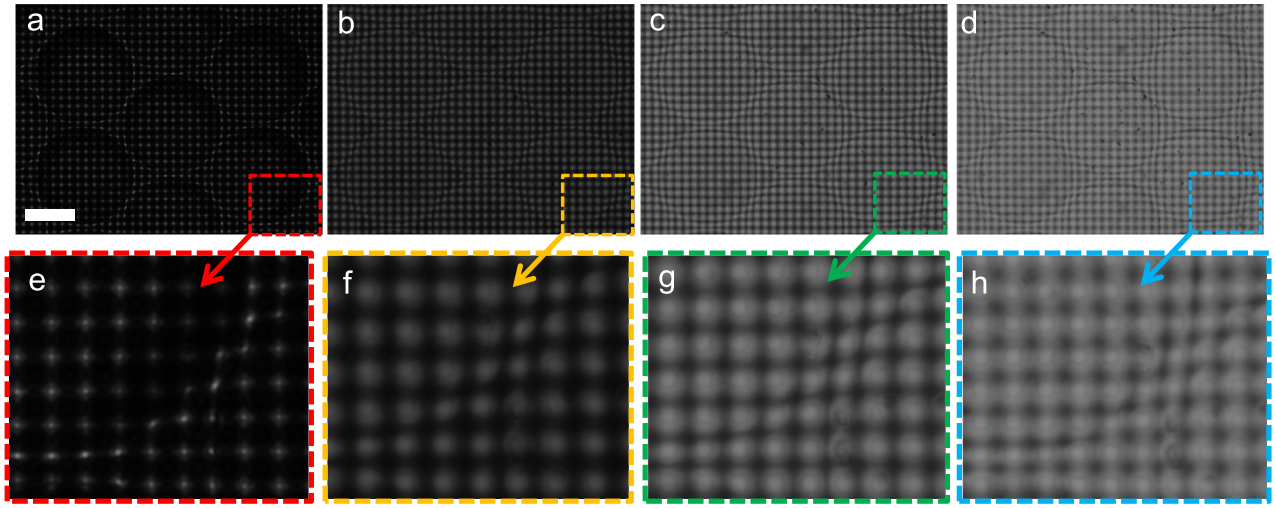

Fig. 6. Image captured with a light field microscope with different illumination NAs. (a) $NA_{cond} = 0.05$; (b) $NA_{cond} = 0.15$; (c) $NA_{cond} = 0.2$; and (d) $NA_{cond} = 0.25$. Scale bar 50 μm.

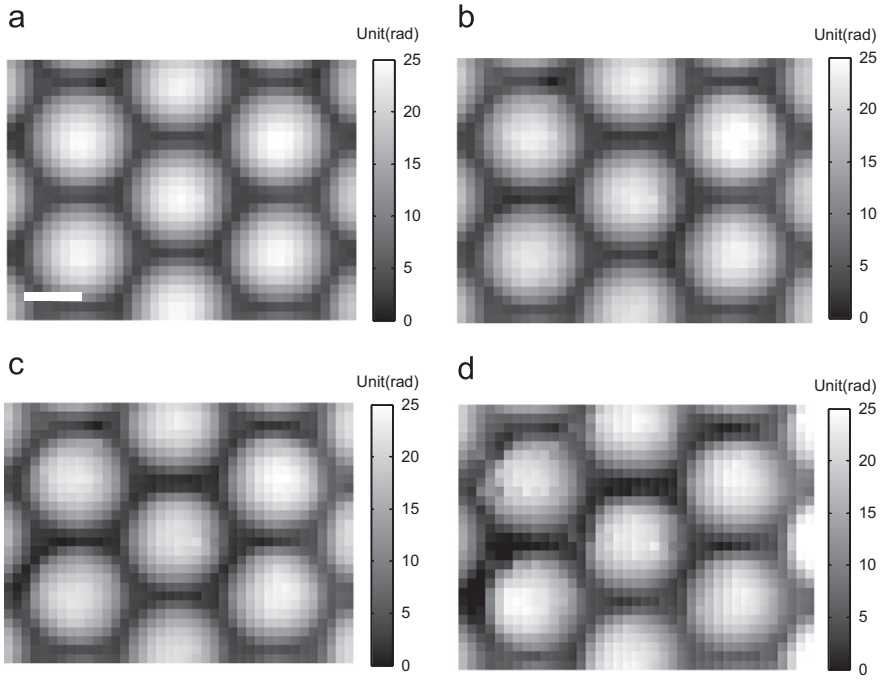

Fig. 7. Phases reconstructed from the light fields with different illumination NAs. (a) $NA_{cond} = 0.05$; (b) $NA_{cond} = 0.15$; (c) $NA_{cond} = 0.2$; (d) $NA_{cond} = 0.25$. Scale bar 50 μm.

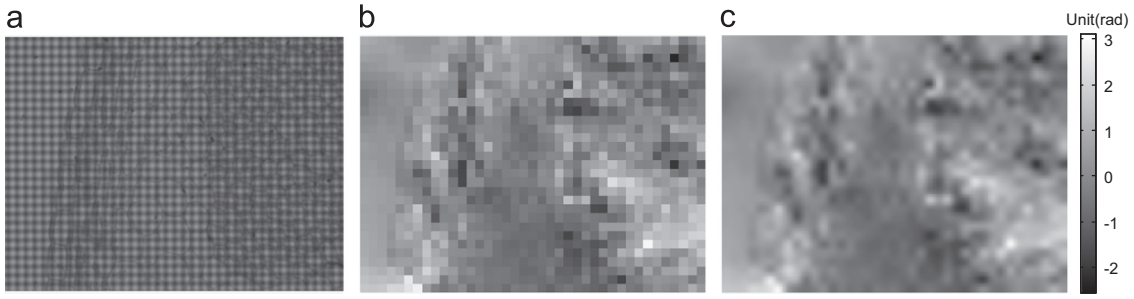

Fig. 8. Results of the stem cell. (a) Raw light field image $NA_{cond} = 0.2$; (b) recovered phase (rad); (c) result after cubic interpolation. Scale bar 50 μm.

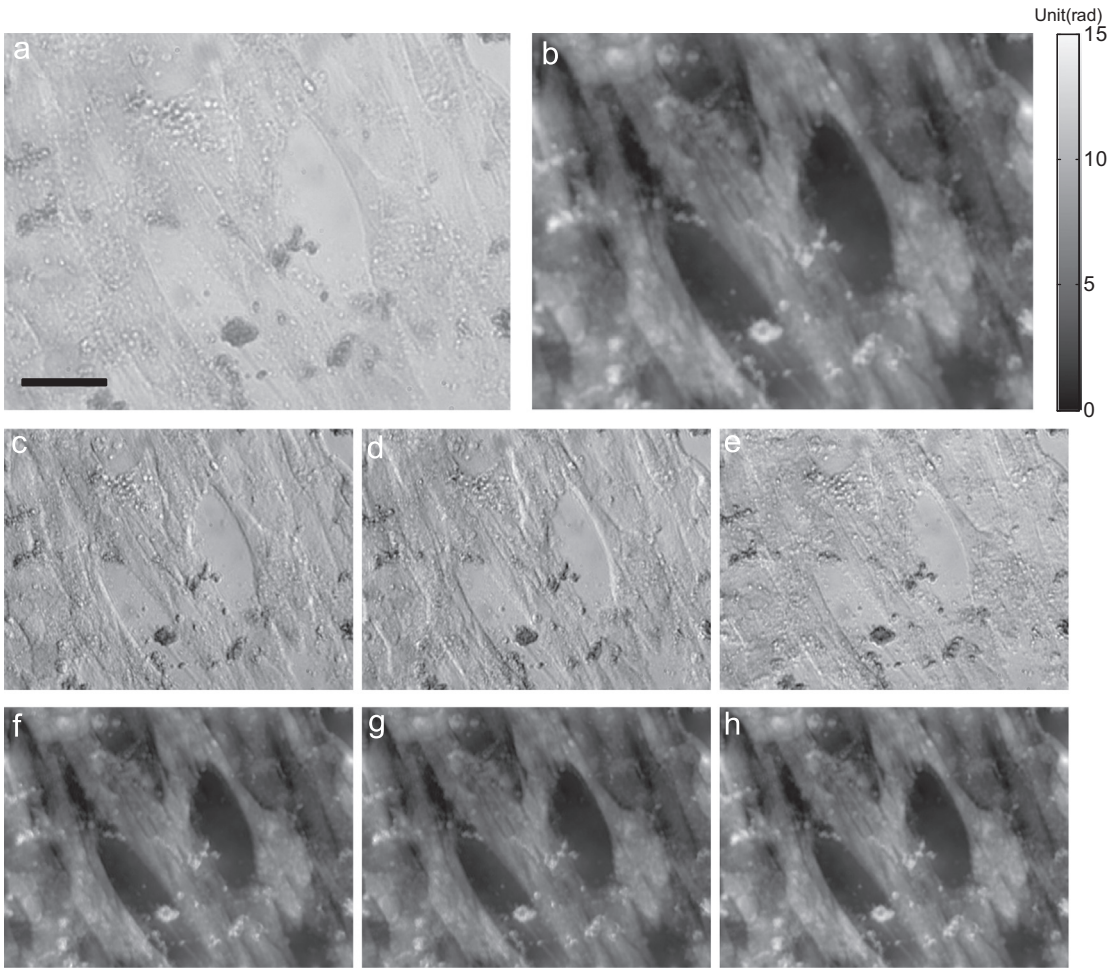

Fig. 9. Computational view synthesis of muscle fiber cells. (a) In-focus bright-field image; (b) quantitative phase image; (c–e) intensity-based viewpoint synthesized images (Media 3); (f–h) phase-based viewpoint synthesized images (Media 4). Scale bar 50 μm.

dimensionality, which totally cover the 2D phase information. Here we consider the inverse of this process: we use the TIE to recover the light field of a slowly varying specimen under spatially stationary illumination computationally.

For a conventional bright-field microscope with a binary circular condenser aperture P_c, the view synthesis based on extracting 2D slices from the 4D light field estimated by Eq. (19) usually performs poorly since the synthesized image for each pixel ($\mathbf{x}$) can only assume two states (neglect the unimportant multiplicative constant c): zero or $I(\mathbf{x})$. By assuming the angular distribution to be Gaussian [42], good perspective shifting effects can be achieved, but it is still groundless and lacks in physical evidence. Such problem is overcome by using Eq. (25) to construct perspective-shifted images, with the effect of the imaging system taken into consideration. To verify the validity of Eq. (25), a simple experiment was conducted based on the same configuration as in Section 7.1. We imaged muscle fibers that regenerated from muscle stem cells in the culture medium (with a $20\times$ $NA_{obj} = 0.45$ objective, $NA_{cond} = 0.2$) to show how our approach can facilitate monitoring label-free biological specimens at a subcellular level with a high resolution. Fig. 9(a) shows the in-focus bright-field image, which shows very low contrast as cells are almost pure phase object. Fig. 9(b) shows the quantitative phase recovered by TIE from which the underlying structure of muscle stem cells is clearly visualized with high contrast. We can easily identify the muscle fibers tightly interlinking and stacking over each other during muscle regeneration, as shown in the bright regions in the phase image [Fig. 9(b)]. With use of Eq. (25), different perspectives of the original scene can be synthesized, as shown in Fig. 9(c)–(e) and animated in

Media 3. The view-synthesized images produce shadow-cast effects that effectively highlight the details present in the specimen without physically moving the source or the specimen. Furthermore, since the perspective-shifted image is reconstructed computationally based on the intensity measurement and the phase recovered by the TIE. The view synthesis can also be performed based on the retrieved phase image instead of the intensity image by simply replacing the intensity $I(\mathbf{x})$ in Eq. (25) with the retrieval phase image $\phi(\mathbf{x})$. This step virtually converts the transmissive object into an absorbing one (the phase is used for direct visualization), and thus, different perspectives of the phase image can also be digitally reconstructed. Since most useful information of the cell is contained in the phase image, the phase-based view synthesis provides a more apparent perspective effect compared with the intensity-based view synthesis, as shown in Fig. 9(f)–(h) and animated in Media 4. The computational nature of the proposed approach provides tremendous flexibilities to realize various types of phase contrast, light field imaging, or their combinations, which was previously impossible with a conventional bright-field microscope.

8. Conclusions and discussions

In summary, we have presented a phase-space formulation of the TIE based on the WDF for the study of phase retrieval and computational imaging under partially coherent illuminations. As it turns out, the phase of partially coherent field in phase space can be described as a scalar potential whose gradient yields the conditional frequency moment of the WDF. Physically, this conditional WDF moment represents the normalized ensemble-averaged transverse Poynting vector, or the centroid of the light field at geometric optics limit. With this generalized definition, the phase of the sample under partially coherent illuminations can be simply retrieved via one-time TIE measurement with limited coherence requirements, provided the source distribution is symmetric about the optical axis. We then demonstrated that partial coherence and the limited imaging pupil effect can be described as a convolution of the illumination WDF or the WDF of the imaging PSF along different dimensions. Such a description allows intuitive understanding as well as quantitative analysis of issues (i.e., coherence, aperture effect) related to TIE phase retrieval under partially coherent illuminations. Furthermore, the WDF serves as a direct bridge between the physical optics and the geometric optics, enabling applications of the TIE to be extended to high-resolution light field imaging for slowly varying specimens, in a purely computational manner. The theoretical analysis has been extensively verified by simulations and experiments.

Finally, it has to be admitted that the view from phase space does not provide anything new to the study of the partial coherence in TIE, as compared with the previous formulations based on correlation functions. This is quite understandable because the correlation functions (mutual intensity, cross-spectral density) form the basis for the definition of the WDF – they both contain equivalent information. However, in many cases, the phase-space representation are more valuable for conceptual reasons than computational ones. It provides an intuitive but rigorous framework that leads to many useful ideas and interpretations, even if the results derived from them can then be expressed in a different (or even simpler) way that bypasses the phase-space picture. With the equivalence of the WDF and light field in phase space, we have demonstrated the tight connections between phase and light field, and the practical applications of the TIE phase retrieval in the field of light field imaging. We anticipate that the phase-space framework will broaden the ambit of the TIE phase measurement, offer new and flexible imaging modalities that were previously not possible using traditional bright-field microscopy, and open up more applications in a wider range of contexts.

Acknowledgments

This work was supported by the the Fundamental Research Funds for the Central Universities of China (30915011318).

Appendix A. Proof of Eq. (13)

For the derivation of Eq. (13), we put the representation of $W_{out}(\mathbf{x},\mathbf{u})$ [Eq. (12)] into the conditional frequency moment [the LHS of Eq. (10)], then the numerator of the result is

$$\int \mathbf{u}W_{out}(\mathbf{x},\mathbf{u})\,d\mathbf{u} = \iint \mathbf{u}W_T(\mathbf{x},\mathbf{x}')W_{in}(\mathbf{x},\mathbf{u}-\mathbf{x}')\,d\mathbf{x}'\,d\mathbf{u}, \tag{26}$$

Interchanging the order of integral gives

$$\begin{aligned}
&\int \mathbf{u}W_{out}(\mathbf{x},\mathbf{u})\,d\mathbf{u}\\
&= \int W_T(\mathbf{x},\mathbf{x}')\int \mathbf{u}W_{in}(\mathbf{x},\mathbf{u}-\mathbf{x}')\,d\mathbf{u}\,d\mathbf{x}'\\
&= \int W_T(\mathbf{x},\mathbf{x}')\int (\mathbf{u}-\mathbf{x}'+\mathbf{x}')W_{in}(\mathbf{x},\mathbf{u}-\mathbf{x}')\,d\mathbf{u}\,d\mathbf{x}'\\
&= \int \mathbf{x}'W_T(\mathbf{x},\mathbf{x}')\,d\mathbf{x}'\int W_{in}(\mathbf{x},\mathbf{u}-\mathbf{x}')\,d\mathbf{u}\\
&\quad + \int W_T(\mathbf{x},\mathbf{x}')\,d\mathbf{x}'\int (\mathbf{u}-\mathbf{x}')W_{in}(\mathbf{x},\mathbf{u}-\mathbf{x}')\,d\mathbf{u}\\
&= \int \mathbf{u}W_T(\mathbf{x},\mathbf{u})\,d\mathbf{u}\int W_{in}(\mathbf{x},\mathbf{u})\,d\mathbf{u}\\
&\quad + \int W_T(\mathbf{x},\mathbf{u})\,d\mathbf{u}\int \mathbf{u}W_{in}(\mathbf{x},\mathbf{u})\,d\mathbf{u}.
\end{aligned} \tag{27}$$

The denominator of the result is

$$\int W_{out}(\mathbf{x},\mathbf{u})\,d\mathbf{u} = \int W_T(\mathbf{x},\mathbf{x}')W_{in}(\mathbf{x},\mathbf{u}-\mathbf{x}')\,d\mathbf{x}'\,d\mathbf{u}. \tag{28}$$

Interchanging the order of integral gives

$$\begin{aligned}
\int W_{out}(\mathbf{x},\mathbf{u})\,d\mathbf{u} &= \int W_T(\mathbf{x},\mathbf{x}')\int W_{in}(\mathbf{x},\mathbf{u}-\mathbf{x}')\,d\mathbf{u}\,d\mathbf{x}'\\
&= \int W_{in}(\mathbf{x},\mathbf{u})\,d\mathbf{u}\int W_T(\mathbf{x},\mathbf{u})\,d\mathbf{u},
\end{aligned} \tag{29}$$

or simply

$$\begin{aligned}
\int W_{out}(\mathbf{x},\mathbf{u})\,d\mathbf{u} &= I_{out}(\mathbf{x})\\
&= I_{in}(\mathbf{x})|\,T(\mathbf{x})\,|^2 = \int W_{in}(\mathbf{x},\mathbf{u})\,d\mathbf{u}\int W_T(\mathbf{x},\mathbf{u})\,d\mathbf{u}.
\end{aligned} \tag{30}$$

Combining above results, we can get Eq. (13):

$$\frac{\int \mathbf{u}W_{out}(\mathbf{x},\mathbf{u})\,d\mathbf{u}}{\int W_{out}(\mathbf{x},\mathbf{u})\,d\mathbf{u}} = \frac{\int \mathbf{u}W_T(\mathbf{x},\mathbf{u})\,d\mathbf{u}}{\int W_T(\mathbf{x},\mathbf{u})\,d\mathbf{u}} + \frac{\int \mathbf{u}W_{in}(\mathbf{x},\mathbf{u})\,d\mathbf{u}}{\int W_{in}(\mathbf{x},\mathbf{u})\,d\mathbf{u}}. \tag{31}$$

Appendix B. Proof of Eq. (17)

For a completely coherent field $U(\mathbf{x}) = A(\mathbf{x})\exp[i\phi(\mathbf{x})]$, e.g. the object is illuminated by a plane monochromatic beam, its WDF can be represented as

$$\begin{aligned}
W(\mathbf{x},\mathbf{u}) &= \int U\left(\mathbf{x}+\frac{\mathbf{x}'}{2}\right)U^*\left(\mathbf{x}+\frac{\mathbf{x}'}{2}\right)\exp(-i2\pi\mathbf{u}\mathbf{x}')\,d\mathbf{x}',\\
&= \int A\left(\mathbf{x}+\frac{\mathbf{x}'}{2}\right)A\left(\mathbf{x}-\frac{\mathbf{x}'}{2}\right)\exp\left[i\phi\left(\mathbf{x}+\frac{\mathbf{x}'}{2}\right)-i\phi\left(\mathbf{x}-\frac{\mathbf{x}'}{2}\right)\right]\\
&\quad\times\exp(-i2\pi\mathbf{u}\mathbf{x}')\,d\mathbf{x}'.
\end{aligned} \tag{32}$$

Employing the Taylor expansion to the amplitude and phase function

$$A\left(\mathbf{x}\pm\frac{\mathbf{x}'}{2}\right)=A(\mathbf{x})\pm\frac{\mathbf{x}'}{2}\cdot\nabla A(\mathbf{x})+O\left(|\nabla|^2A(\mathbf{x})\right); \tag{33}$$

$$\phi\left(\mathbf{x}\pm\frac{\mathbf{x}'}{2}\right)=\phi(\mathbf{x})\pm\frac{\mathbf{x}'}{2}\cdot\nabla\phi(\mathbf{x})+O\left(|\nabla|^2\phi(\mathbf{x})\right). \tag{34}$$

If we assume a slowly varying object, the higher order (>2) terms can be ignored, yielding

$$\phi\left(\mathbf{x}+\frac{\mathbf{x}'}{2}\right)-\phi\left(\mathbf{x}-\frac{\mathbf{x}'}{2}\right)\approx\mathbf{x}'\cdot\nabla\phi; \tag{35}$$

$$A\left(\mathbf{x}+\frac{\mathbf{x}'}{2}\right)A\left(\mathbf{x}-\frac{\mathbf{x}'}{2}\right)\approx I(\mathbf{x}). \tag{36}$$

Substituting Eqs. (35) and (36) into Eq. (32), we can get Eq. (17):

$$\begin{aligned}W(\mathbf{x},\mathbf{u})&=I(\mathbf{x})\int\exp(i\mathbf{x}'\cdot\nabla\phi)\exp(-i2\pi\mathbf{u}\mathbf{x}')\,d\mathbf{x}'\\&=I(\mathbf{x})\delta\left[\mathbf{u}-\frac{1}{2\pi}\nabla\phi(\mathbf{x})\right].\end{aligned} \tag{37}$$

Appendix C. Supplementary material

Supplementary data associated with this paper can be found in the online version at http://dx.doi.org/10.1016/j.optlaseng.2015.03.006. This work was supported by the the Fundamental Research Funds for the Central Universities of China (30915011318).

References

[1] Teague MR. Deterministic phase retrieval: a Green's function solution. J Opt Soc Am 1983;73:1434–41.
[2] Nugent KA. Coherent methods in the X-ray sciences. Adv Phys 2010;59:1–99.
[3] Bajt S, Barty A, Nugent K, McCartney M, Wall M, Paganin D. Quantitative phase-sensitive imaging in a transmission electron microscope. Ultramicroscopy 2000;83:67–73.
[4] Allman B, McMahon P, Nugent K, Paganin D, Jacobson D, Arif M, et al. Phase radiography with neutrons. Nature 2000;408:158–9.
[5] Streibl N. Phase imaging by the transport equation of intensity. Opt Commun 1984;49:6–10.
[6] Barty A, Nugent KA, Paganin D, Roberts A. Quantitative optical phase microscopy. Opt Lett 1998;23:817–9.
[7] Waller L, Kou SS, Sheppard CJR, Barbastathis G. Phase from chromatic aberrations. Opt Express 2010;18:22817–25.
[8] Kou SS, Waller L, Barbastathis G, Marquet P, Depeursinge C, Sheppard CJR. Quantitative phase restoration by direct inversion using the optical transfer function. Opt Lett 2011;36:2671–3.
[9] Waller L. Phase imaging with partially coherent light. Proc SPIE 2013;8589 85890K-1–6.
[10] Zuo C, Chen Q, Qu W, Asundi A. Noninterferometric single-shot quantitative phase microscopy. Opt Lett 2013;38:3538–41.
[11] Paganin D, Nugent KA. Noninterferometric single-shot quantitative phase microscopy. Opt Lett 2013;38:3538–41.
[12] Gureyev TE, Paganin DM, Stevenson AW, Mayo SC, Wilkins SW. Generalized eikonal of partially coherent beams and its use in quantitative imaging. Phys Rev Lett 2004;93:068103.
[13] Zysk AM, Schoonover RW, Carney PS, Anastasio MA. Transport of intensity and spectrum for partially coherent fields. Opt Lett 2010;35:2239–41.
[14] Petruccelli JC, Tian L, Barbastathis G. The transport of intensity equation for optical path length recovery using partially coherent illumination. Opt Express 2013;21:14430–41.
[15] Adelson EH, Bergen JR. The plenoptic function and the elements of early vision. Comput Models Vis Process 1991;1.
[16] Levoy M, Hanrahan P. Light field rendering. In: Proceedings of the 23rd annual conference on computer graphics and interactive techniques, SIGGRAPH '96. New York, NY, USA: ACM; 1996. p. 31–42.
[17] Ng R, Levoy M, Brédif M, Duval G, Horowitz M, Hanrahan P. Light field photography with a hand-held plenoptic camera. Computer science technical report CSTR 2; 2005.
[18] Bastiaans MJ. Application of the Wigner distribution function to partially coherent light. J Opt Soc Am A 1986;3:1227–38.
[19] Walther A. Radiometry and coherence. J Opt Soc Am 1968;58:1256–9.
[20] Gureyev TE, Roberts A, Nugent KA. Partially coherent fields, the transport-of-intensity equation, and phase uniqueness. J Opt Soc Am A 1995;12:1942–6.
[21] Semichaevsky A, Testorf M. Phase-space interpretation of deterministic phase retrieval. J Opt Soc Am A 2004;21:2173–9.
[22] Boashash B. Estimating and interpreting the instantaneous frequency of a signal. i. fundamentals. Proc IEEE 1992;80:520–38.
[23] Bastiaans M. The Wigner distribution function applied to optical signals and systems. Opt Commun 1978;25:26–30.
[24] Zuo C, Chen Q, Asundi A. Boundary-artifact-free phase retrieval with the transport of intensity equation: fast solution with use of discrete cosine transform. Opt Express 2014;22:9220–44.
[25] Zhang Z, Levoy M. Wigner distributions and how they relate to the light field. In: IEEE international conference on computational photography (ICCP); 2009. p. 1–10.
[26] Winston R, Welford WT. Geometrical vector flux and some new nonimaging concentrators. J Opt Soc Am 1979;69:532–6.
[27] Dragoman D. Phase-space interferences as the source of negative values of the Wigner distribution function. J Opt Soc Am A 2000;17:2481–5.
[28] Bastiaans MJ. Uncertainty principle for partially coherent light. J Opt Soc Am 1983;73:251–5.
[29] Gureyev T, Nesterets Y, Paganin D, Pogany A, Wilkins S. Linear algorithms for phase retrieval in the fresnel region. 2. Partially coherent illumination. Opt Commun 2006;259:569–80.
[30] Tian L, Zhang Z, Petruccelli JC, Barbastathis G. Wigner function measurement using a lenslet array. Opt Express 2013;21:10511–25.
[31] Nugent KA. Wave field determination using three-dimensional intensity information. Phys Rev Lett 1992;68:2261–4.
[32] Raymer MG, Beck M, McAlister D. Complex wave-field reconstruction using phase-space tomography. Phys Rev Lett 1994;72:1137–40.
[33] Ferraro P, Nicola SD, Finizio A, Coppola G, Grilli S, Magro C, et al. Compensation of the inherent wave front curvature in digital holographic coherent microscopy for quantitative phase-contrast imaging. Appl Opt 2003;42:1938–46.
[34] Paganin D, Gueryev TE, Mayo SC, Stevenson AW, Nesterets YI, Wilkins SW. X-ray omni microscopy. J Microsc 2004;214:315–27.
[35] Zuo C, Chen Q, Qu W, Asundi A. High-speed transport-of-intensity phase microscopy with an electrically tunable lens. Opt Express 2013;21:24060–75.
[36] Friberg AT. On the existence of a radiance function for finite planar sources of arbitrary states of coherence. J Opt Soc Am 1979;69:192–8.
[37] Oh SB, Kashyap S, Garg R, Chandran S, Raskar R. Rendering wave effects with augmented light field. Comput Graph Forum 2010;29:507–16.
[38] Alonso M. The connection between rays and waves. In: Osten W, editor. Fringe 2013. Berlin, Heidelberg: Springer; 2014. p. 457–64.
[39] Platt B, Shack R. History and principles of shack-hartmann wavefront sensing. J Refract Surg 2001;17:S5737.
[40] Waller L, Situ G, Fleischer JW. Phase-space measurement and coherence synthesis of optical beams. Nat Photonics 2012;6:474–9.
[41] Zuo C, Chen Q, Asundi A. Light field moment imaging: comment. Opt Lett 2014;39:654.
[42] Orth A, Crozier KB. Light field moment imaging. Opt Lett 2013;38:2666–8.
[43] Zuo C, Chen Q, Li H, Qu W, Asundi A. Boundary-artifact-free phase retrieval with the transport of intensity equation ii: applications to microlens characterization. Opt Express 2014;22:18310–24.
[44] Colomb T, Montfort F, Kühn J, Aspert N, Cuche E, Marian A, et al. Numerical parametric lens for shifting, magnification, and complete aberration compensation in digital holographic microscopy. J Opt Soc Am A 2006;23:3177–90.
[45] Zuo C, Chen Q, Qu W, Asundi A. Phase aberration compensation in digital holographic microscopy based on principal component analysis. Opt Lett 2013;38:1724–6.